

Single-Particle Properties of a Two-Dimensional Fermi Liquid at finite Frequencies and Temperatures

Jungsoo Kim and D. Coffey

Department of Physics, State University of New York, Buffalo, NY 14260

(November 5, 2018)

We review the leading momentum, frequency and temperature dependences of the single particle self-energy and the corresponding term in the entropy of a two dimensional Fermi liquid (FL) with a free particle spectrum. We calculate the corrections to these leading dependences for the paramagnon model and the electron gas and find that the leading dependences are limited to regions of energy and temperature which decrease with decreasing number density of fermions. This can make it difficult to identify the frequency and temperature dependent characteristics of a FL ground state in experimental quantities in low density systems even when complications of band structure and other degrees of freedom are absent. This is an important consideration when the normal state properties of the undoped cuprate superconductors are analyzed.

I. INTRODUCTION

The 2D nature of the cuprate oxide superconductors and the fact that their normal state properties do not exhibit leading FL behavior have lead to the suggestion that the ground state is not a FL. In a FL the resistivity should follow a T^2 dependence as the temperature T goes to zero in the absence of impurities and it has been argued that the absence of this characteristic FL behavior in several experiments for the cuprate superconductors [1–4] is evidence that there is a qualitative difference between the normal state of cuprates and that in the other metallic system. Anderson [5] has argued that the ground state of cuprates is close to the one-dimensional system in which the elementary excitations are collective modes, spinons and holons, with spin and charge degrees of freedom decoupled as in the 1D Luttinger liquid. Varma *et al.* [6] have put forward a model in which the weight in the quasiparticle pole vanishes logarithmically at $p = p_f$. This is similar to case of the Luttinger liquid although in that case the weight is the quasiparticle poles at the Fermi surface vanishes as $z_F \sim (p - p_f)^\alpha, 1 > \alpha > 0$ [7]. The stability of the FL ground state has been investigated in perturbation theory [8–11], by renormalization group calculations [12] and bosonization of the fermions [13,14]. These approaches have not revealed any sign of FL breakdown other than due to the instabilities of FL ground state familiar from three-dimensional (3D) case : BCS, CDW or SDW. Metzner *et al.* have reviewed work on the role of strong forward scattering in determining the ground state of Fermi systems in different dimensions. [15] As they point out for short interactions or the Coulomb interaction the properties of Fermi systems in dimensions greater than one are those of usual Fermi liquid. More recently Castellani *et al.* [16] have suggested that the anomalous normal state properties of the cuprates are due to quantum critical points associated with antiferromagnetism and charge density wave instabilities in different doping ranges. In the region of a quantum critical point temperature provides the only energy scale which it is argued is consistent with data on the cuprates.

An alternative explanation is that, although the ground state develops from FL at $T = 0$, the characteristic FL temperature dependence is restricted to low temperatures compared to the high superconducting transition temperature, T_c , or compared to small energy scales given by large variations in the density of states due to bandstructure effects such as a Van Hove singularity [17].

The energy and temperature dependent characteristics of a FL arise from quasiparticle interactions. Corrections to these dependences also arise from the quasiparticle interactions themselves at energy and temperature scales which depend on the nature of interactions. The corrections limit the characteristic FL dependences to the vicinity of the Fermi surface and to low temperature even in the absence of bandstructure and other effects. We investigate the corrections to these leading FL energy and temperature dependences using a parabolic band in order to isolate the effects of bandstructure. It is useful to investigate the leading corrections for the FL with a simplest model where non-essential complications are absent. Here we calculate $\Sigma'(p, E)$ and $\Sigma''(p, E)$ for the paramagnon model [18] and the electron gas. The paramagnon model describes the physical system close to a ferromagnetic instability where the self-energy contribution comes from incoherent long-wavelength spin fluctuations through particle-hole (ph) channel. The closer the system is to the instability the stronger are the leading corrections to FL behavior since they come from the long wavelength limit of the effective interaction. This makes the paramagnon model ideal for investigating corrections and the regions of energies and temperatures over which they can characterize calculated quantities. Since the 2D electron liquid has recently been used to investigate the corrections to FL behavior, we also calculate these corrections for the Coulomb interaction. In these calculations $\Sigma(p, E)$ is approximated by the ph channel contribution. Unlike 3D this channel remains important at low densities in 2D so that our results can also be applied to low densities.

The difference between 2D and 3D is that the density of states for a parabolic band at the Fermi surface is independent of density in 2D. Consequently repeated scattering in the ph channel remains important at low density in 2D [20].

In the section II we introduce the paramagnon model and in the section III discuss the results for the single-particle self-energy and thermodynamic properties. In the section IV we discuss the same kind of corrections for the 2D electron gas. We give our conclusions in section V.

II. MODEL

To calculate the leading corrections to the single-particle self-energy we first use a short range interaction between fermions. The Hamiltonian is

$$H = \sum_{\mathbf{p},\sigma} \xi_{\mathbf{p}} c_{\mathbf{p},\sigma}^\dagger c_{\mathbf{p},\sigma} + \sum_{\mathbf{p},\mathbf{q},\sigma,\sigma'} I(\mathbf{q}) c_{\mathbf{p},\sigma}^\dagger c_{\mathbf{p}',\sigma'} c_{\mathbf{p}'-\mathbf{q},\sigma'}^\dagger c_{\mathbf{p}+\mathbf{q},\sigma} \quad (1)$$

where $\xi_p = (p^2 - p_f^2)/2m$, m is the mass of the fermions, p_f is the Fermi momentum and I is the strength of the interaction with a cutoff, q_c . This model, called the paramagnon model, was used by Engelsberg *et al.* [18] to calculate the corrections to the linear temperature dependences in specific heat of normal liquid 3He . Within this model the leading corrections to FL behavior come from low energy long wavelength paramagnons. The importance of paramagnons in liquid 3He was suggested by the enhancement of the observed static paramagnetic susceptibility and were shown to provide an explanation of the size of corrections to the linear temperature dependence of the specific heat. The single-particle self-energy is given by the repeated scattering of ph pairs which leads to an effective interaction, $V^{eff}(\mathbf{q}, \omega)$.

$$\Sigma(\mathbf{p}, \imath E_n) = -T \sum_{\mathbf{q}, \omega_l} G(\mathbf{p} - \mathbf{q}, \imath E_n - \omega_l) V^{eff}(\mathbf{q}, \omega_l) \quad (2)$$

where $G(\mathbf{p}, \imath E_n)$ is the unperturbed temperature Green function and ω_l is Bose Matsubara frequencies. $V^{eff}(\mathbf{q}, \omega)$ has two independent channels, the symmetric (s) and the antisymmetric (a) channels corresponding to spin exchanges of 0 or 1 and is given by

$$V^{eff}(\mathbf{q}, \omega) = \frac{1}{2} \frac{V_s^2 \chi(\mathbf{q}, \omega)}{1 - V_s \chi(\mathbf{q}, \omega)} + \frac{3}{2} \frac{V_a^2 \chi(\mathbf{q}, \omega)}{1 - V_a \chi(\mathbf{q}, \omega)} \quad (3)$$

where $V_s = I$ and $V_a = -I$. $\chi(\mathbf{q}, \omega)$ is the polarization function for a 2D parabolic band [19]. At $T = 0$ the self-energy contributions from the real and imaginary part on shell ($E = \xi_p$) is

$$\begin{aligned} \Sigma(\mathbf{p}, \xi_p) &= \sum_{\mathbf{q}} [\Theta(\xi_{\mathbf{p}} - \xi_{\mathbf{p}-\mathbf{q}}) - \Theta(-\xi_{\mathbf{p}-\mathbf{q}})] V^{eff}(\mathbf{q}, \xi_{\mathbf{p}} - \xi_{\mathbf{p}-\mathbf{q}}) \\ &+ \int_{-\infty}^{\infty} \frac{d\eta}{2\pi} \sum_{\mathbf{q}} G(\mathbf{p} - \mathbf{q}, \xi_{\mathbf{p}} - \imath\eta) V^{eff}(\mathbf{q}, \imath\eta) \end{aligned} \quad (4)$$

with $\chi(\mathbf{q}, \omega) = \chi'(\mathbf{q}, \omega) + \imath\chi''(\mathbf{q}, \omega)$ in $V_{eff}(\mathbf{q}, \omega)$. The leading corrections in $\Sigma(p, E)$ of interest here comes from the long-wavelength limit and are contained in the first term since the second term, the line integral along the imaginary frequency axis, $\omega = \imath\eta$, does not contribute to the energy dependence in the long wavelength limit. The line integral in the equation (4) does not contribute to the $\Sigma''(p, E)$ since the imaginary part of the integrand is odd in η and gives contributions to $\Sigma'(p, \xi_p)$ which are proportional to q_c^2 .

III. RESULTS

A. Self-Energy At Zero Temperature

The leading dependence on ξ_p in the imaginary part of self-energy in $\Sigma(\mathbf{p}, E) = \Sigma'(\mathbf{p}, E) + \imath\Sigma''(\mathbf{p}, E)$ on shell is

$$\Sigma''(\mathbf{p}, \xi_p) = \beta \xi_p^2 \ln \left| \frac{\xi_{\mathbf{p}}}{\xi_0} \right| + O(\xi_p^4) \quad (5)$$

where β is independent of the direction for a parabolic band and given by

$$\beta = - \int_0^1 \frac{d\mu}{\sqrt{1-\mu^2}} \left(\frac{1}{2} \frac{A_s^3}{[(1-\mu^2) + (A_s\mu)^2]} + \frac{3}{2} \frac{A_a^3}{[(1-\mu^2) + (A_a\mu)^2]} \right) \quad (6)$$

$$\approx - \frac{(1 + \bar{I} + \bar{I}^2)}{(1 - \bar{I}^2)^2} \frac{\bar{I}^2}{4E_f},$$

$A_s = \frac{\bar{I}}{1+\bar{I}}$, $A_a = \frac{\bar{I}}{1-\bar{I}}$ and $\bar{I} = N(0)I$ where $N(0) = m/2\pi\hbar$ is the density of states at the Fermi surface for a 2D parabolic band for up or down spins. The real part of the self-energy for a parabolic band is

$$\Sigma'(\mathbf{p}, \xi_{\mathbf{p}}) = -\alpha\xi_{\mathbf{p}} - \frac{\pi}{2}\beta\xi_{\mathbf{p}}|\xi_{\mathbf{p}}| - \gamma|\xi_{\mathbf{p}}|^{5/2} + O(\xi_{\mathbf{p}}^3) \quad (7)$$

where for the paramagnon model,

$$\alpha \approx \frac{(2 + \bar{I})}{(1 - \bar{I}^2)} \frac{\bar{I}^2 \min[q_c, 2p_f]}{\pi p_f} \quad (8a)$$

$$\gamma \approx \frac{\bar{I}}{4\pi E_f^{3/2}} \quad (8b)$$

where $E_f = p_f^2/2m$ and $\xi_0 \propto p_f$ for $q_c > 2p_f$ and $\xi_0 \propto q_c$ otherwise [20]. The logarithmic behavior is restricted to $|\xi_p| < \xi_0$. In the RPA approximation the largest contribution comes from the antisymmetric channel since the contribution of the channel is enhanced by a $1/(1 - \bar{I})^2$ factor in the case of a repulsive interaction. The generic FL behavior in $\Sigma''(p, \xi_p)$ is shown in the figure 1 with a log-fit. The figure 2 shows an interaction \bar{I} dependence in the logarithmic scale of ξ_p and q_c dependence. The cut-off energy ξ_0 depends only on q_c and the slope β depends on \bar{I} . The q-sum in the equation (4) has a limit of $\min[q_c, 2p_f]$, so that the log-fit for $q_c = 3.0p_f$ and $5.0p_f$ has the same cut off in the log dependence. The log fit is good to within 10 percent up to $\xi_p = 0.2E_f$ which, however, depends on q_c . The $\xi_p|\xi_p|$ term in $\Sigma'(p, \xi_p)$ is related to the $\xi_p^2 \ln |\xi_p|$ term in the imaginary part through the Kramers-Kronig relation [11] and also depends only on long wavelength properties. In the figure 3 the $\xi_p|\xi_p|$ term has been isolated in the logarithmic scale, so that the slope 2 indicates ξ_p^2 in $\ln |\Sigma' + \alpha\xi_p|$. This contribution comes from the dependence of $V^{eff}(q, \omega)$ on the variable $s = \omega/qv_f$ [21] where s is the variable which appears in $\chi(\mathbf{q}, \omega)$ in the long-wavelength limit

$$\lim_{\mathbf{q} \rightarrow 0} \chi(q, \omega) = \chi(s) = N(0) \left[-1 + \frac{s}{\sqrt{s^2 - 1}} \Theta(|s| - 1) + i \frac{s}{\sqrt{1 - s^2}} \Theta(1 - |s|) \right]. \quad (9)$$

As in the $\Sigma''(p, \xi_p)$, the coefficient is independent of q_c and the log fit survives up to $\xi_p \approx \xi_0$. The term is present both for $\xi_p > 0$ and $\xi_p < 0$. The intercept point of vertical axis shows the coefficient $\frac{\pi}{2}\beta$ and the curve for $\xi_p < 0$ ends at $\xi = -E_f$ in $\ln |\xi_p|$. The $|\xi_p|^{5/2}$ term is the leading zero sound contribution. This term has a corresponding $(\xi - \xi_{th})^{3/2}$ term in $\Sigma''(p, \xi_p)$ [20], where $\xi_{th} = (v_{zs} - v_f)$, determined by the velocity of the zero-sound mode, $v_{zs} = [(1 + \bar{I})/\sqrt{1 + 2\bar{I}}]v_f$.

In 3D the leading dependence in $\Sigma''(p, \xi_p)$ is ξ_p^2 and the leading correction to this, $|\xi_p|^3$, corresponds to the term $\xi_p^2 \ln \xi_p$ in 2D. The $|\xi_p|^3$ depends only on long wavelength behavior [22] and has a corresponding $\xi_p^3 \ln |\frac{\xi_p}{\xi_0}|$ term in $\Sigma'(p, \xi_p)$. The cut-off in the log, ξ_0 , depends on both $\bar{I} = N(0)I$ and q_c because of the stronger q dependence in real part of $\chi^{3D}(q, \omega)$. The magnitude of these $\xi_p^2 \ln \xi_p$ and $\xi_p|\xi_p|$ terms in 2D and the $|\xi_p^3|$ and $\xi_p^3 \ln \xi_p$ terms in 3D are enhanced by repeated scattering of ph pairs. The strength of the repeated scattering depends on the coupling constant, \bar{I} , which is independent of p_f in 2D but goes to zero in 3D as $p_f \rightarrow 0$. As a result unlike the case in 3D, where the ph channel is not important for low densities, the enhancement is independent of density in 2D and the results derived here for 2D remain the leading corrections even in low densities. However both in 2D and 3D $\Sigma(p, E) \rightarrow 0$ as the phase space for holes vanishes. The leading correction term of 2D FL is limited to a small energy region which vanishes as p_f decreases in the low density limit.

The dependences of $\Sigma(p, E)$ on the variables, p and E , are very different. For instance $\Sigma''(p, E)$ has a $E^2 \ln \frac{|E|}{E_{\pm}}$ behavior only for $p = p_f$, where $E_+ = E_- = \xi_0$ are cutoffs for $E > 0$ and $E < 0$ respectively. In the figure 4 and the figure 5 we show $\Sigma'(p, E)$ and $\Sigma''(p, E)$ vs. E for $p = p_f$ and $1.1p_f$. As p goes away from p_f , the structure of the self-energy vanishes inside the Fermi surface (for $p < p_f$ the structure vanishes outside the surface) due to the

step function in the zero temperature self-energy expression in the equation (4) and so there is a threshold in the self-energy for $|E| < |\xi_{\mathbf{p}-\mathbf{q}}|_{min}$. The sharp threshold effect is absent for interaction without a cutoff, q_c . However if $V^{eff}(q, \omega)$ falls off with increasing q then there is an effective q_c and associated with that there is an effective cutoff in E beyond which $\Sigma(p, E)$ is reduced in magnitude. The most direct probe of the E dependence of $\Sigma(p, E)$ is in angle resolved photoemission spectroscopy in which the spectral density is measured. The quasi-particle peak in the data depends on the E dependence of $\Sigma(p, E)$ and has been analyzed for the cuprate superconductors in both the normal and superconducting state [23]. It has been found that the linewidth of quasi-particle peak does not vary as E^2 which has been pointed as not being the FL dependence [24]. The strong p and E dependence of $\Sigma(p, E)$ found here for a simple parabolic band shows that deviations from a simple E^2 dependence are to be expected. This is especially the case for cuprates with strong bandstructure effects and quasi-particle interactions giving rise to low energy spin fluctuations [25].

B. Self-Energy at Finite Temperature

At finite temperature $\Sigma''(p, \xi_p)$ is

$$\Sigma''(\mathbf{p}, \xi_{\mathbf{p}}) = - \sum_{\mathbf{q}} [f(-\xi_{\mathbf{p}-\mathbf{q}}) + n(\xi_{\mathbf{p}} - \xi_{\mathbf{p}-\mathbf{q}})] ImV^{eff}(\mathbf{q}, \xi_{\mathbf{p}} - \xi_{\mathbf{p}-\mathbf{q}}) \quad (10)$$

where n and f are Bose and Fermi distribution functions respectively. The temperature dependence of $\Sigma''(p_f, \xi_{p_f})$ is plotted for different values of q_c in the figure 6. $\Sigma''(p, \xi_p)$ calculated with $\chi(q, \omega)$ evaluated at zero temperature is the solid lines and with the temperature dependent $\chi''(q, \omega, T)$ are the circles. As can be seen from figure 6, the temperature dependence in the $\chi''(q, \omega, T)$ does not affect the cut-off T_0 since the $\chi(q, \omega, T)$ does not vary much respect to T for $T \ll E_f$ in the long wave length limit. The leading dependence of $\Sigma''(p, \xi_p)$ on p and T is given by

$$\Sigma''(p, \xi_p) = \beta(\xi_p^2 + \pi^2 T^2) \ln(max[\xi_p, T]/T_0) \quad (11)$$

which is shown on the figure 7. The zero temperature and finite temperature cutoffs, ξ_0 and T_0 , are shown in figure 8. They have similar values and increase for $q_c \leq 2p_f$ and are independent of q_c for larger values of q_c . Although the self-energy at finite temperature does not have explicit step functions as in zero temperature case, the finite temperature cutoffs are independent of $q_c \geq 2p_f$ since the log behavior comes from low temperatures. Since both ξ_0 and T_0 are proportional to p_f at low densities the leading FL behavior in the temperature case is also limited to a region which depends on the density of the system.

As T increases beyond the degenerate temperature region, the Bose distribution term dominates the contribution from the Fermi Dirac distribution term in the equation (10). In the high temperature limit $\Sigma''(p_f, \xi_{p_f})$ is approximated by

$$\Sigma''(p_f, \xi_{p_f}) \approx -\beta \frac{8min[q_c, 2p_f]}{p_f} T + O\left(\frac{1}{T}\right) \quad (12)$$

where the linear term in T comes from the Bose contribution. $\Sigma''(p_f, \xi_{p_f})$ has been graphed in two ways, $\Sigma''(p_f, \xi_{p_f})/T^2$ vs. $\ln T$ and $\ln[\Sigma''(p_f, \xi_{p_f})]$ vs. $\ln T$ in the figure 9 for $q_c = 0.1p_f$ and $q_c = 1.0p_f$. The dashed lines are the logarithmic and linear temperature dependence determined from equations (11) and (12). The size of the crossover region from the low temperature limit to the high temperature limit is small as can be seen in the figure and is from $T = 0.02E_f/k_B$ to $T = 0.03E_f/k_B$. This is estimated by considering 10 percent deviation from the fits. Although the linear T dependence comes from the high temperature limit, as soon as the temperature dependence behavior leaves the $T^2 \ln T$ behavior it tends to reach the linear temperature dependence rapidly. Since T_0 is proportional to density the leading FL behavior survives in a low temperature region which shrinks with decreasing density and the linear high temperature behavior is followed at lower and lower temperatures. The size of crossover also decreases with density. The same behavior is seen in 3D with similar crossover properties. Consequently this behavior is not determined by band-structure or low dimensionality and it may be misleading to refer to it as Luttinger-like [17].

C. Thermodynamic Properties

The contribution from quasiparticle interactions to the thermodynamic potential, $\Delta\Omega$, can be calculated by linked cluster expansion [26]. After analytic continuation to the real ω axis $\Delta\Omega$ can be split up into $\Delta\Omega_{qp}$ from a quasiparticle contribution and $\Delta\Omega_{cm}$ from a collective modes;

$$\begin{aligned}\Delta\Omega(T) &= -T \sum_{\omega_n} \sum_{\mathbf{q}} \int_0^1 \frac{d\eta}{\eta} \chi(\eta, q, i\omega_n) V^{eff}(\eta, q, i\omega_n) \\ &= \Delta\Omega_{qp} + \Delta\Omega_{cm}.\end{aligned}\tag{13}$$

First, $\Delta\Omega_{qp}$ is

$$\Delta\Omega_{qp}(T) = \sum_{|\mathbf{q}| < \mathbf{q}_c} \int_0^\infty \frac{d\omega}{\pi} n(\omega) [F(\mathbf{q}, \omega) + 2I^2 \chi''(\mathbf{q}, \omega)],\tag{14}$$

where

$$F(q, \omega) = \sum_{\lambda=s,a} \nu_\lambda \tan^{-1} \left[\frac{-V_\lambda \chi''(q, \omega)}{1 - V_\lambda \chi'(q, \omega)} \right].\tag{15}$$

By taking a derivative $\Delta\Omega_{qp}$ respect to T , the shift in the entropy, ΔS_{qp} , is

$$\begin{aligned}\Delta S_{qp}(T) &= - \sum_{|\mathbf{q}| < \mathbf{q}_c} \int_0^\infty \frac{\partial n(\omega)}{\partial T} [F(\mathbf{q}, \omega) + 2I^2 \chi''(\mathbf{q}, \omega)] \\ &\quad - \sum_{|\mathbf{q}| < \mathbf{q}_c} \int_0^\infty \frac{d\omega}{2\pi} n(\omega) \left[\frac{\partial F(\mathbf{q}, \omega)}{\partial T} + 2I^2 \frac{\partial \chi''(\mathbf{q}, \omega)}{\partial T} \right]\end{aligned}\tag{16}$$

The second term is negligible since, as shown in the previous section, the temperature dependence in $\chi(\mathbf{q}, \omega)$ is weak in the long-wavelength limit. The temperature dependence in entropy mainly comes from the first term. The entropy from quasiparticle contribution is

$$\Delta S_{qp}(T) = \Gamma_1 T + \Gamma_2 T^2 + O(T^3),\tag{17}$$

$$\Gamma_1 = \frac{\pi}{6T_f} (A_s + A_a) \frac{q_c}{p_f}\tag{18a}$$

$$\Gamma_2 = -\frac{6\zeta(3)n}{\pi T_F^2} \beta\tag{18b}$$

where n is density of particles and ζ is the Riemann zeta function [11]. The figure 10 shows T^2 dependence for $q_c = 0.1p_f$ and $q_c = p_f$. The q_c dependent linear T term has been subtracted. As in the figure 3, the slope of the term does not depend on q_c . This term can also be calculated by including $\Sigma'(p, \xi_p)$ in the quasiparticle spectrum and using the expression for the entropy of non-interacting gas. The quasiparticle spectrum has the $\xi_p |\xi_p|$ term which is directly connected to T^2 term in the entropy [11]. This T^2 describes the corrections to the $\Gamma_1 T$ dependence in ΔS_{qp} to better than 10 percent up to a temperature T_S for entropy in the figure 10 which follows the same trend as T_0 ($\sim \xi_0$) in the figure 8 but is smaller.

The collective mode contribution, $\Delta\Omega_{cm}(T)$, is given by the zero-sound pole in the symmetric channel in $V^{eff}(\mathbf{q}, \omega)$. Taking derivative respect to T , one has a T^2 dependence in ΔS_{cm} . In the figure 10 ΔS_{cm} is compared with ΔS_{qp} . The contribution to T^2 from the collective mode is about a percent of the quasi-particle contribution.

The calculations discussed so far using the paramagnon model have shown that FL behavior is limited to regions of low energy and temperature which shrink with decreasing density. The cutoffs, ξ_0 and T_0 , are determined by the finite momentum dependence of the quasiparticle interaction. We now turn to the 2D electron gas which has recently been of experimental and theoretical interest.

IV. 2D ELECTRON GAS

Murphy *et al.* [27] have compared their data on the tunneling conductance in 2D quantum well systems to the expression for the single particle life time expression derived by Giuliani and Quinn [28] using long wavelength approximation and found quantitative agreement if they multiplied this expression by 6.3. Jungwirth *et al.* [29] have

investigated the same calculation with an effective interaction suggested by MacDonald *et al.* [30] between fermions with a static long wavelength limit in V^{eff} and they obtained good fits to the data. We calculate the imaginary part of self-energy for the quasi-particles in n-type doped GaAs using the RPA.

Instead of applying static approximation calculated in RPA with local corrections in $V^{eff}(q, \omega)$, we use the frequency dependent effective interaction,

$$V_q^{eff}(\mathbf{q}, \omega) = \frac{I_q^2 \chi(\mathbf{q}, \omega)}{1 - I_q \chi(\mathbf{q}, \omega)} \quad (19)$$

where $I_q = 2\pi e^2 / \epsilon_s q$ or $\bar{I}_q = 2\pi e^2 N(0) / \epsilon_s q = 0.02 \text{\AA}^{-1} / q$ [27] ($N(0)$ is density of states at Fermi level). For GaAs the static dielectric constant, ϵ_s , is about 10 and $m^*/m = 0.067$. The only free parameter is p_f . As pointed out in the discussion of the contact interaction the coefficient of the $(\xi_p^2 + \pi^2 T^2) \ln(\max[\xi_p, T]/T_0)$ dependence in $\Sigma''(p, \xi_p)$ is determined by the long wavelength properties of $V^{eff}(q, \omega)$.

There are two contributions to $\Sigma(p, E)$. One comes from the interaction of the quasi-particles with incoherent ph pairs. This contribution gives the leading FL corrections and was discussed in detail above for the contact interaction. The second contribution comes from the interaction of quasi-particles with the plasmon mode. Although it does not contribute to the leading p and E dependence of $\Sigma''(p, E)$, it is comparable in magnitude to that from the incoherent ph pairs at finite E . These contributions and $\Sigma''(p, E)$ are plotted in figure 11 for $p = p_f$ and $p = 1.1p_f$ at $T = 0$. $\Sigma''(p_f, E)$ is symmetric and leads to a spectral density which is symmetric in the figure 12. For $p \neq p_f$ $\Sigma''(p, E)$ is no longer symmetric in E as was pointed out in the discussion of the contact interaction.

Using the parameters for quasi-particles in n-type doped GaAs quantum wells temperature dependence of $\Sigma''(p, E = \xi_p)$ is shown in figure 13 for $n = 1.6 \times 10^{11} \text{cm}^{-2}$ which gives $p_f = 0.01 \text{\AA}^{-1}$ and $E_f = \frac{p_f^2}{2m^*} = 5.7 \text{meV}$. As in the contact interaction case there is a cross over from $T^2 \ln T$ to linear T behavior which depends on density. $T^2 \ln T$ dependence is followed for $T_1 < 8K$ and T dependence for $T_2 > 156K$ for $p_f = 0.01 \text{\AA}^{-1}$ system. These values of T_1 and T_2 were determined by requiring the $\Sigma''(p_f, \xi_{p_f})$ to fit the $T^2 \ln T$ and T dependences to 10 percent. The $T^2 \ln T$ dependence in the Coulomb interaction is also limited by low density limit as in contact interaction case. The cross over region (T_1 to T_2) has been estimated for different densities and is shown in table 1. The size of this region decreases with decreasing density system as in the contact interaction case but is larger.

Quasiparticle interactions of an isotropic electron gas do not contribute to the transport relaxation time [26]. However the results of the calculations discussed here suggest that it is important to take into account the p and E dependences of $\Sigma''(p, E)$ and the plasmon contribution when comparing calculations of single particle properties in the 2D electron gas with experiment data.

V. CONCLUSION AND SUMMARY

We calculated the corrections to FL behavior in the single particle self-energies and in entropy using a contact and Coulomb interaction. We demonstrated that these corrections take the forms, $\xi_p |\xi_p|$ in $\Sigma'(p, \xi_p)$ and $\xi_p^2 \ln |\xi_p|$ in $\Sigma''(p, \xi_p)$, in a region close to the Fermi surface which shrinks with decreasing density and increasing temperature. In particular we have shown that at finite temperatures $\Sigma''(p_f, \xi_{p_f})$ rapidly goes over to a linear T dependence even for a parabolic band. This type of linear temperature leads to a resistivity $\propto T$ which has been taken as evidence against a FL ground state in the cuprate superconductors. Our results suggest that an alternative explanation may be that the temperature below which FL behavior is seen is below the superconducting transition temperature. This has also been suggested by Aristov *et al.* [17] on the basis of band-structure effects in 2D Hubbard Hamiltonian.

This point has been addressed by Boebinger *et al.* [31] who have applied magnetic fields to suppress superconductivity in transport measurements on the cuprates at low temperatures. It is claimed that this reveals the normal state. They find that the non-FL behaviors persists. However recent work by Chan *et al.* [32] suggests that single particle properties of 2D electron systems are very sensitive to modest applied magnetic fields. They found that a pseudogap appears in the density of states in applied fields. A similar resistivity was also found in transport properties of 2D electron system in semiconductor hetero-structures by Simonian *et al.* [33]. We will address the influence of magnetic fields on 2D FL in a forthcoming paper.

This work was supported by the New York State Institute for Superconductivity(NYSIS).

- [1] Y. Iye *et al.*, in “*Physical Properties of High Temperature Superconductors*”, Vol.3(Ed D. M. Ginsberg), World Scientific, Singapore (1992)
- [2] H. Takagi, B. Batlogg, H.L.Kao, J. Kwo, R.J. Cava, J.J. Krajewski and W.F. Peck, Jr., Phys. Rev. Lett. **69**, 2975 (1992).
- [3] Y. Ando, G.S. Boebinger, A. Passer, T. Kimura and K. Kishio, Phys. Rev. Lett. **75**, 4662 (1995).
- [4] T. Timusk and D.B. Tanner, in “*High-Temperature Superconductors*”, Vol.I(Ed D.M. Ginsberg), World Scientific, Singapore (1989).
- [5] P.W. Anderson, Phys. Rev. Lett. **64**, 1839 (1990) and **65**, 2306 (1991).
- [6] C.M. Varma, P.B. Littlewood, S. Schmitt-Rank, E. Abrahams and A.E. Ruckenstein, Phys. Rev. Lett **63**, 1996 (1989).
- [7] J. Voit, Rep. Prog. Phys. **58**, 977 (1995).
- [8] J.R. Engelbrecht and M. Randeria, Phys. Rev. Lett. **65**,1032 (1990) and Phys. Rev. B **45**, 12419 (1992).
- [9] H. Fukuyama, Y. Hasegawa and O. Narikiyo, J. Phys. Soc. Jap. **60**, 2013 (1991).
- [10] J.W. Serene and D.W. Hess, Phys. Rev. B **44**, 3391 (1991).
- [11] D. Coffey and K.S. Bedell, Phys. Rev. Lett. **71**, 1043(1993).
- [12] R. Shankar, Physics A **177**, 530 (1991); Rev. Mod. Phys. **66**, 129 (1994).
- [13] A. Houghton, H.J. Kwon and J.B. Marston, Phys. Rev. B **48**, 7790 (1993); Phys. Rev. B **50**, 1351 (1994).
- [14] A.H. Castro Neto and E. Fradkin, Phys. Rev. B **49**, 10877 (1994).
- [15] W. Metzner, C. Castellani and C. Di Castro, preprint (1997); LANL cond-mat/9701012.
- [16] C.Castellani, C. Di Castro and M. Grilli, preprint (1997); LANL cond-mat/9702112.
- [17] D.N. Aristov, S.V. Maleyev and A.G. Yashenkin, Phys. Rev. B **48**, 3527 (1993).
- [18] S. Doniach and S. Engelsberg, Phys. Rev. Lett. **17**, 750 (1966).
- [19] D. Stern, Phys. Rev. Lett. **18**, 546 (1967).
- [20] J. Kim and D. Coffey, Phil. Mag. B **74**, 477 (1996).
- [21] In the second order calculation the $\xi_p|\xi_p|$ term exists for $p > p_f$ because it comes from $|s| = |p\mu/p_f| > 1$ in the real part of $\chi(s)$ where $\mu = \hat{q} \cdot \hat{p}$. However $|p\mu/p_f| < 1$ for $p < p_f$. As a result the on-shell self-energy calculated for second order can be a misleading indication of the ξ_p dependence.
- [22] G. Baym and C.J. Pethick, in “*The Physics of Liquid and Solid Helium*”, edited by K.H. Bennemann and J.B. Ketterson (Wiley, New York, 1978).
- [23] Z.X. Shen, D.S. Dessau, B.O. Wells and D.M. King, J. Phys. Chem. Solids, **54**, 1169 (1993).
- [24] Z.X. Shen and J.R. Schrieffer, Phys. Rev. Lett. **78**, 1771 (1997).
- [25] K. Kouznetsov and L. Coffey, Phys. Rev. B **54**, 3617 (1996).
- [26] G.D. Mahan, “*Many-Particle Physics*”, 2nd ed, Plenum, New York (1990).
- [27] S.Q. Murphy, J.P. Eisenstein, L.N. Pfeiffer and K.W. West, Phys. Rev. B **52**, 14825 (1996).
- [28] G.F. Giuliani and J.J. Quinn, Phys. Rev. B **26**, 4421 (1982).
- [29] T. Jungwirth and A.H. MacDonald, Phys. Rev. B **53**, 7403 (1996).
- [30] A.H. MacDonald and D.J.W. Geldart, Can. J. Phys. **60**, 1016 (1982).
- [31] Y. Ando, G.S. Boebinger and A. Passner, Phys. Rev. Lett. **75**, 4662 (1995).
- [32] H.B. Chan, P.I. Glicofridis, R.C. Ashoori and M.R. Melloch, Preprint (1997); LANL cond-mat/9702088.
- [33] D. Simonian, S.V. Kravchenko and M.P. Sarachik, Preprint (1997); LANL cond-mat/9704071.

TABLE I. Crossover temperatures from $T^2 \ln T$ behavior (T_1) to T behavior (T_2) in the temperature dependence of $\Sigma''(p_f, \xi_{p_f})$ of the 2D electron gas. T_1 and T_2 are defined by 10 percent deviation from the fitting curves.

density ($\times 10^{11} \text{ cm}^{-2}$)	T_1 (K)	T_2 (K)
6.37	25	231
3.58	20	236
3.12	16	258
1.93	12	185
1.59	8	156

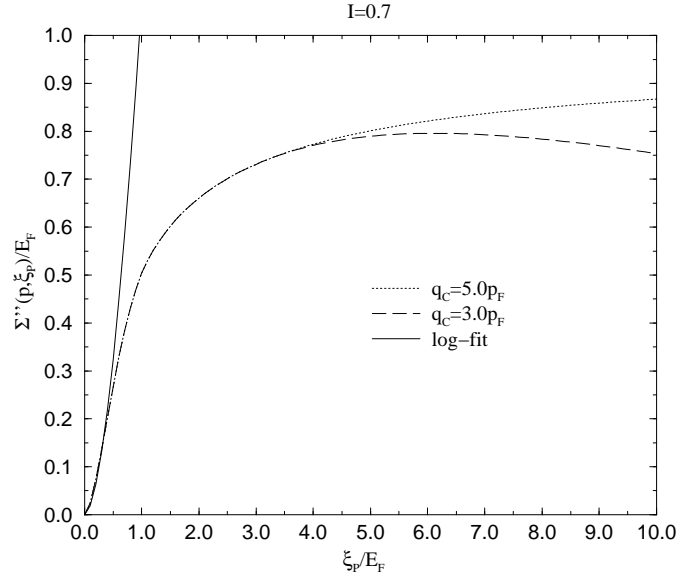


FIG. 1. $\Sigma''(p, \xi_p)$ on a linear energy scale for $q_c = 5.0p_f$ and $3.0p_f$ when $\bar{I} = 0.7$.

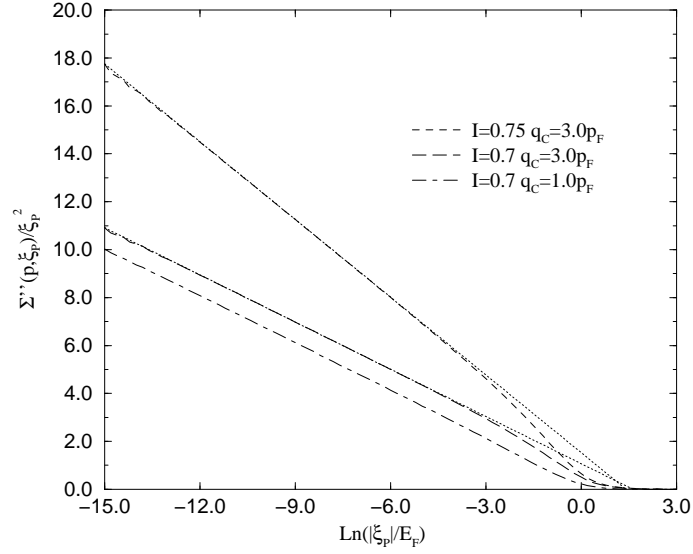


FIG. 2. $\Sigma''(p, \xi_p)$ on a logarithmic energy scale for parabolic band (for the same q_c 's but different \bar{I} 's the cut-offs, ξ_0 , are the same. The energies are in the unit of E_f).

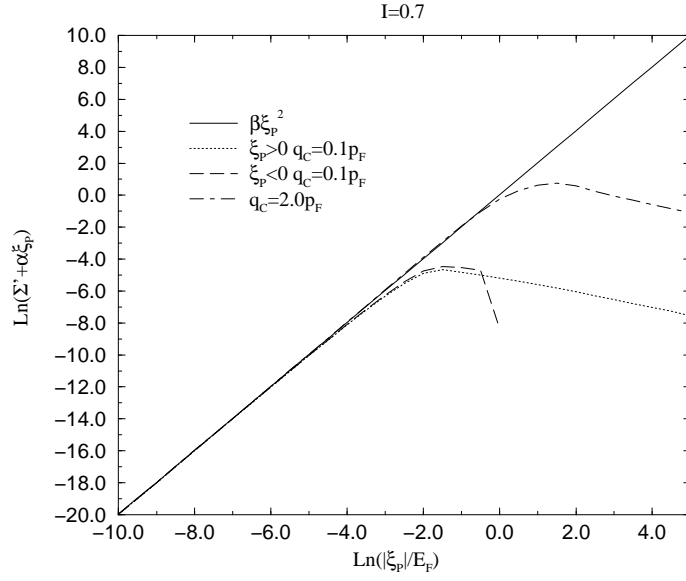


FIG. 3. The $\xi_p |\xi_p|$ term in the real part of $\Sigma(p, \xi_p)$. (Energies are in the unit of E_f .)

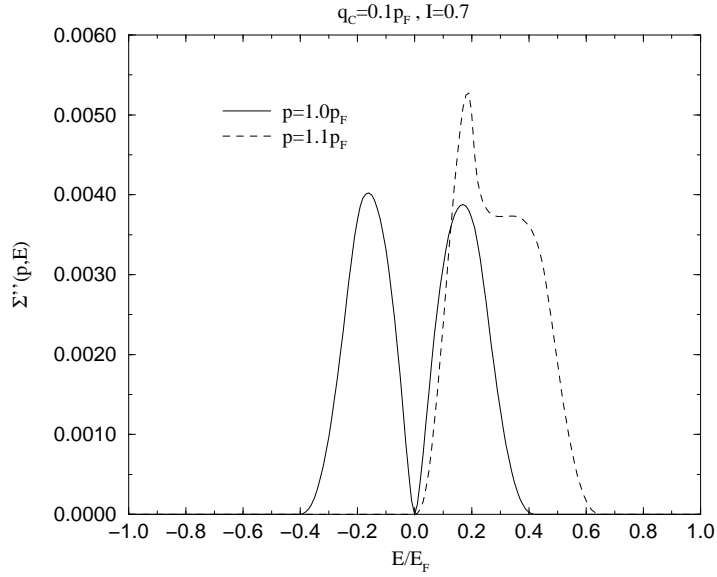


FIG. 4. $\Sigma''(p, E)$, off-shell self-energy, for $p = p_f$ and $1.1 p_f$. $\Sigma''(p, E)$ has a very different form from $\Sigma''(p, \xi_p)$. The structure of $\Sigma''(p, E)$ has q_c dependence through step function in equation (4).

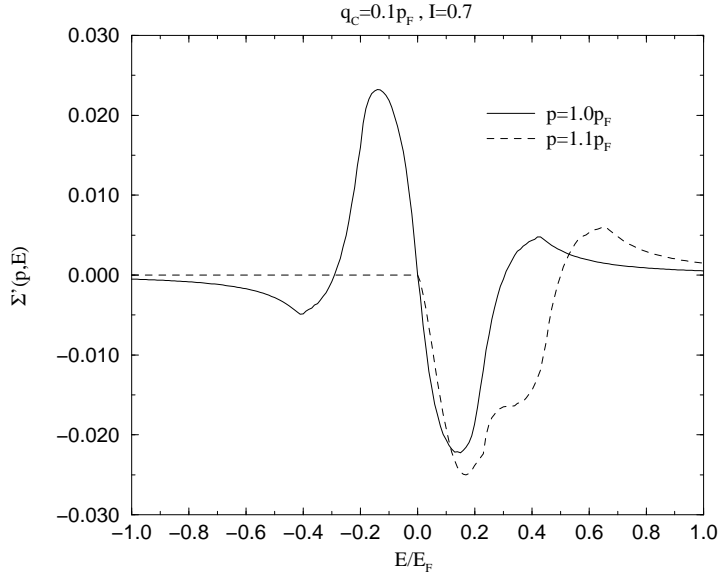


FIG. 5. $\Sigma'(p, E)$, off-shell real part of self-energy, for $p = p_f$ and $1.1p_f$. The structure of $\Sigma'(p, E)$ also has q_c dependence through step function in equation (4).

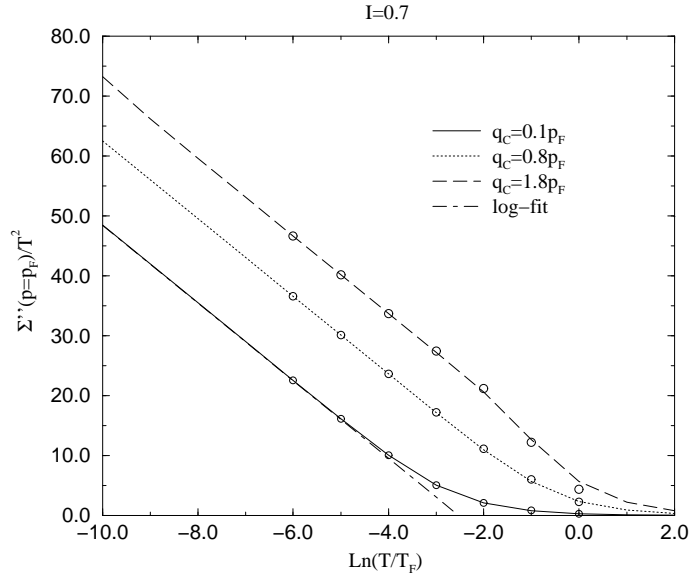


FIG. 6. The temperature dependent $\Sigma''(p_f, \xi_{p_f})$ on a logarithmic T scale (The circles calculated by the temperature dependent $\chi''(q, \omega)$.)

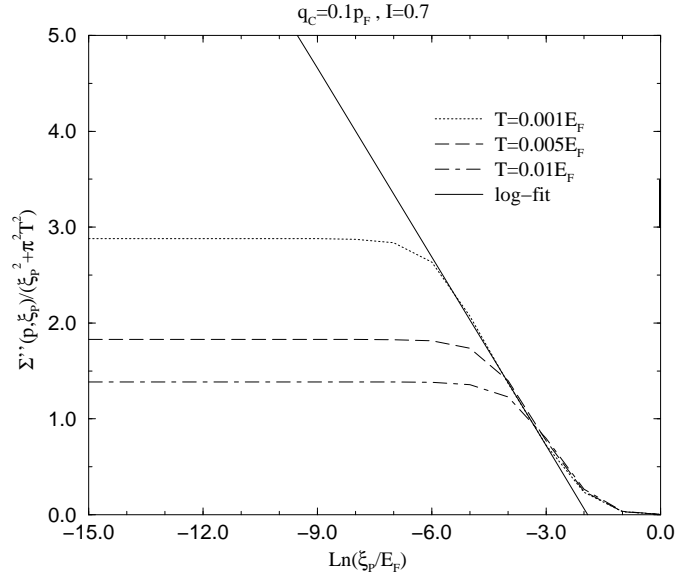


FIG. 7. The temperature dependent $\Sigma''(p, \xi_p)$ on a logarithmic energy scale at $T = 0.001E_f$, $0.005E_f$ and $0.01E_f$.

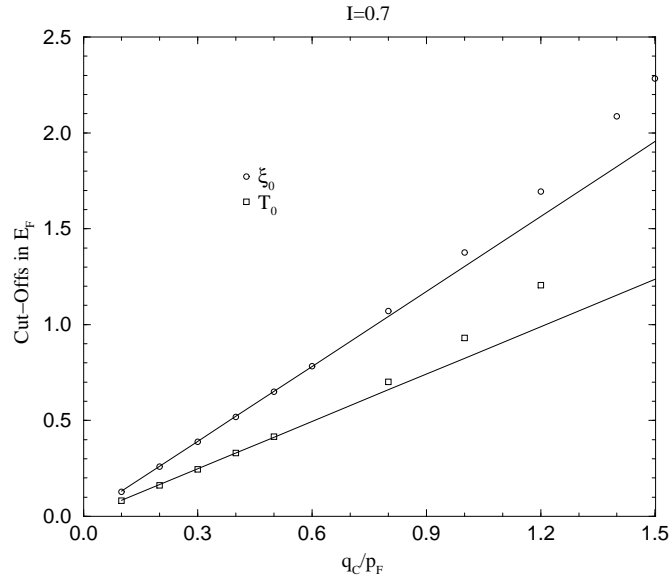


FIG. 8. The cut-offs ξ_0 from $\Sigma''(p, \xi_p)$ at zero temperature and T_0 from $\Sigma(p = p_f, \xi_p, T)$, as q_c approaches zero ξ_0 and T_0 have linear dependence in q_c .

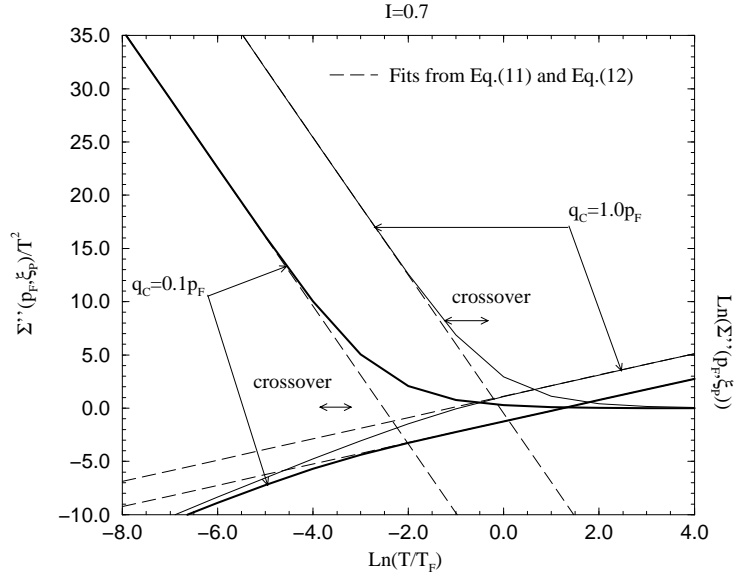


FIG. 9. $T^2 \ln T$ and linear T dependence in $\Sigma''(p_f, \xi_p)$. The dotted lines are the fits from equations (11) and (12). The left solid line is $\Sigma(p_f, \xi_p)/T^2$ and the right is $\ln[\Sigma(p_f, \xi_p)]$. The crossover from the $T^2 \ln T$ to T behaviors has been marked by \leftrightarrow . The width of the cross region is $\sim 0.01E_f$ for $q_c = 0.1p_f$.

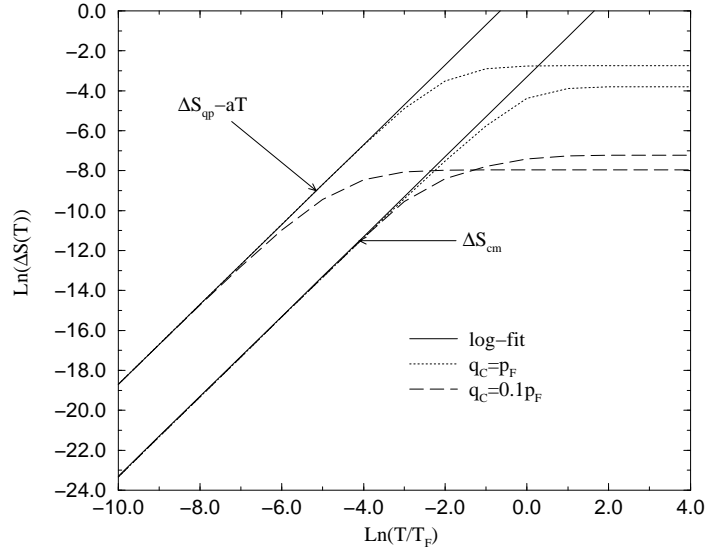


FIG. 10. T^2 contributions in entropy from quasi-particle scattering with the continuum and with the collective mode in entropy; the solid line is the T^2 fit, the T dependence term has been subtracted from $\Delta S_{qp}(T)$. The continuum contribution is $\sim 10^2$ larger than the zero sound contribution.

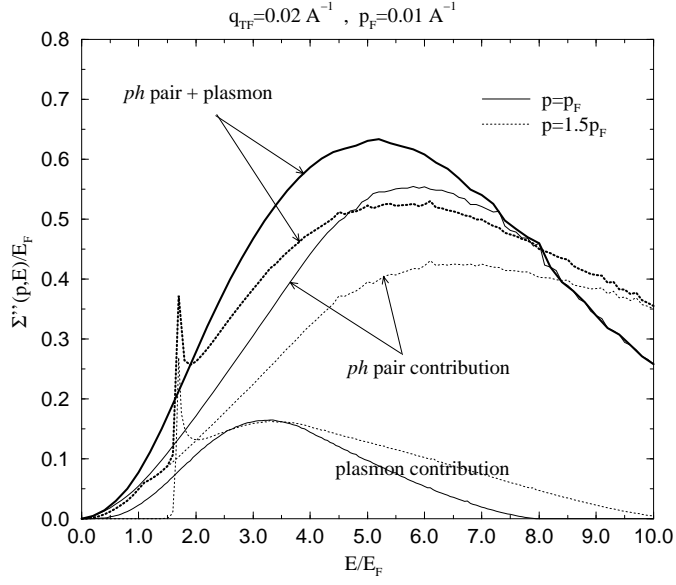


FIG. 11. The incoherent ph pair and plasmon contributions to $\Sigma''(p, E)$ for $p = p_f$ and $p = 1.1p_f$.

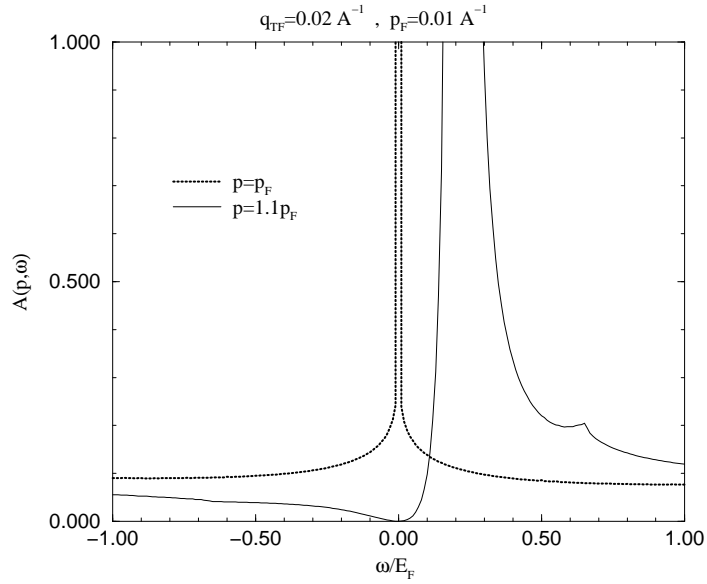


FIG. 12. The spectral function, $A(p, \omega)$, when $p = p_f$ and $p = 1.1p_f$. As p is away from the Fermi surface, asymmetry occurs. $A(p, \omega)$ in the figure has ph and plasmon contributions. The feature at $\omega/E_f \approx 0.6$ comes from the plasmon contribution.

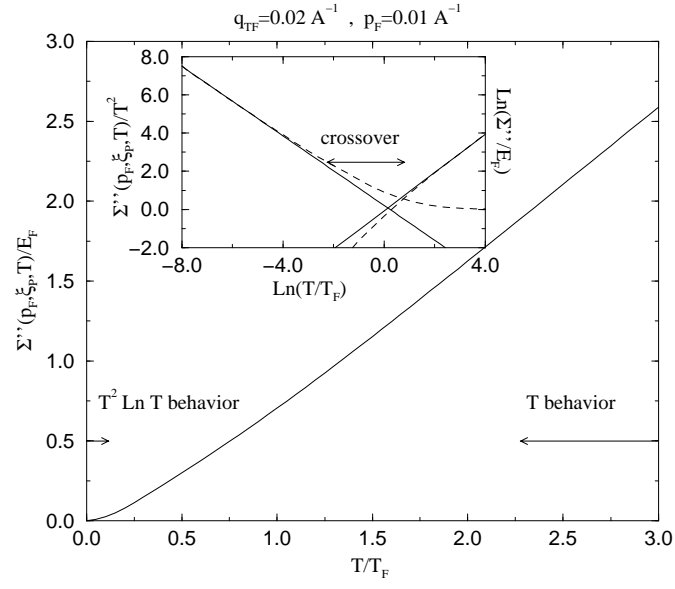


FIG. 13. Extended plot of $\Sigma''(p_f, \xi_{p_f}, T)$ for 2D quasi-particles for n-typed doped GaAs system with $n = 1.6 \times 10^{11} \text{ cm}^{-2}$. Inset is plotted by logarithmic scale and shows crossover.